The EMBO Journal vol.9 no.6 pp.1749 – 1756, 1990

Cloning and expression of a human voltage-gated potassium channel. A novel member of the RCK potassium channel family

Andrew Grupe, Klaus Hasso Schröter[1], Johann Peter Ruppersberg[1], Martin Stocker, Thorsten Drewes, Synnöve Beckh[2] and Olaf Pongs

Ruhr-Universität Bochum, Lehrstuhl für Biochemie, D-4630 Bochum, [1]Max-Planck-Institut für medizinische Forschung, Abteilung Zellphysiologie, D-6900 Heidelberg and [2]Max-Planck Institut für biophys. Chemie, Abteilung Membranbiophysik, D-3400 Göttingen, FRG

Communicated by B.Sakmann

We have isolated and characterized a human cDNA (HBK2) that is homologous to a novel member (RCK2) of the K^+ channel RCK gene family expressed in rat brain. RCK2 mRNA was detected predominantly in midbrain areas and brainstem. The primary sequences of the HBK2/RCK2 K^+ channel proteins exhibit major differences to other members of the RCK gene family. The bend region between segments S1 and S2 is unusually long and does not contain the N-glycosylation site commonly found in this region. They might be O-glycosylated instead. Functional characterization of the HBK2/RCK2 K^+ channels in *Xenopus laevis* oocytes following microinjection in *in vitro* transcribed HBK2 or RCK2 cRNA showed that the HBK2/RCK2 proteins form voltage-gated K^+ channels with novel functional and pharmacological properties. These channels are different to RCK1, RCK3, RCK4 and RCK5 K^+ channels.

Key words: channel diversity/gene family/K^+ channels/mammalian brain/mRNA expression

Introduction

Voltage-gated K^+ channels are transmembrane proteins that seem to be present in almost every eukaryotic cell (Rudy, 1988). K^+ channels provide the outward current that inward Na^+ and Ca^{2+} currents must overcome to depolarize the membrane (Hille, 1984). As a result of this, K^+ channels play an important role in regulating excitability of cells and in setting the resting potential of the membrane. It is now clear that voltage-gated K^+ channels are encoded by distinct, but related multigene families giving rise to the diversity of voltage-gated K^+ channels found in excitable cells (Butler *et al.*, 1989; Frech *et al.*, 1989; Stühmer *et al.*, 1989b). Cloning and sequencing of four separate cDNAs has revealed four members of a gene family (RCK) that are highly homologous in structure, but distinct in their pharmacological and electrophysiological properties (Stühmer *et al.*, 1989b). This shows that relatively small variations in amino acid sequences of K^+ channel forming proteins can be responsible for diverse voltage-gated K^+ channels. Therefore, isolation of other K^+ channel forming proteins is relevant for a molecular understanding of the basic structure of voltage-gated K^+ channels and for an understanding of the amino acid changes that underly the differences in electrophysiological and pharmacological properties.

Recently, the polymerase chain reaction (PCR) method was applied to find RCK homologous sequences in the human genome (Kamb *et al.*, 1989). The results showed that the human genome encodes K^+ channel protein sequences that are very similar to the RCK protein sequences. This observation suggested that the human genome encodes an RCK-like multigene family. In characterizing members of the human RCK-like multigene family, we have isolated and sequenced a cDNA from which a novel K^+ channel forming protein was derived (HBK2). The corresponding rat cDNA was also isolated and characterized for comparison. [RCK2: it should be noted that a cDNA clone that corresponded to the sequence of RCK1 cDNA from nucleotides +245 to +1864 (Baumann *et al.*, 1988) originally was designated RCK2. According to our new nomenclature, each number following the abbreviation RCK denotes a different K^+ channel protein expressed in the rat brain; therefore we have changed the nomenclature of the old RCK2 clone described by our laboratory to RCK1a.] The functional properties of the channels formed by the HBK2 and RCK2 proteins measured after injection of the respective cRNAs into *Xenopus laevis* oocytes showed that these proteins assemble into very similar voltage-gated K^+ channels with functional and pharmacological characteristics distinct from the hitherto known RCK K^+ channels. The RCK2 channel and its human homologue HBK2 add another member to the RCK multigene family, thus increasing the diversity of voltage-gated K^+ channels derived from this K^+ channel family.

Results

Cloning a human K^+ channel cDNA

Previously, we have used *Drosophila Shaker* and RCK1 cDNA probes to isolate homologous rat cDNAs encoding K^+ channel forming (RCK) proteins (Baumann *et al.*, 1988; Stühmer *et al.*, 1989). By analogy, we have hybridized, with an RCK3 cDNA probe, a human fetal cDNA library under conditions of low stringency and have screened for homologous cDNAs encoding RCK-related proteins. Several hybridizing clones were isolated and sequenced. These clones corresponded to overlapping cDNAs encoding a human K^+ channel subunit homologous to members of the RCK-protein family. The deduced open reading frame consisted of 490 amino acids, but was apparently incomplete for the amino-terminal end of the derived protein. As we were not able to isolate another cDNA with which we could have completed the open reading frame, we isolated the corresponding genomic DNA. Genomic DNA digested with various restriction enzymes was hybridized with radio-

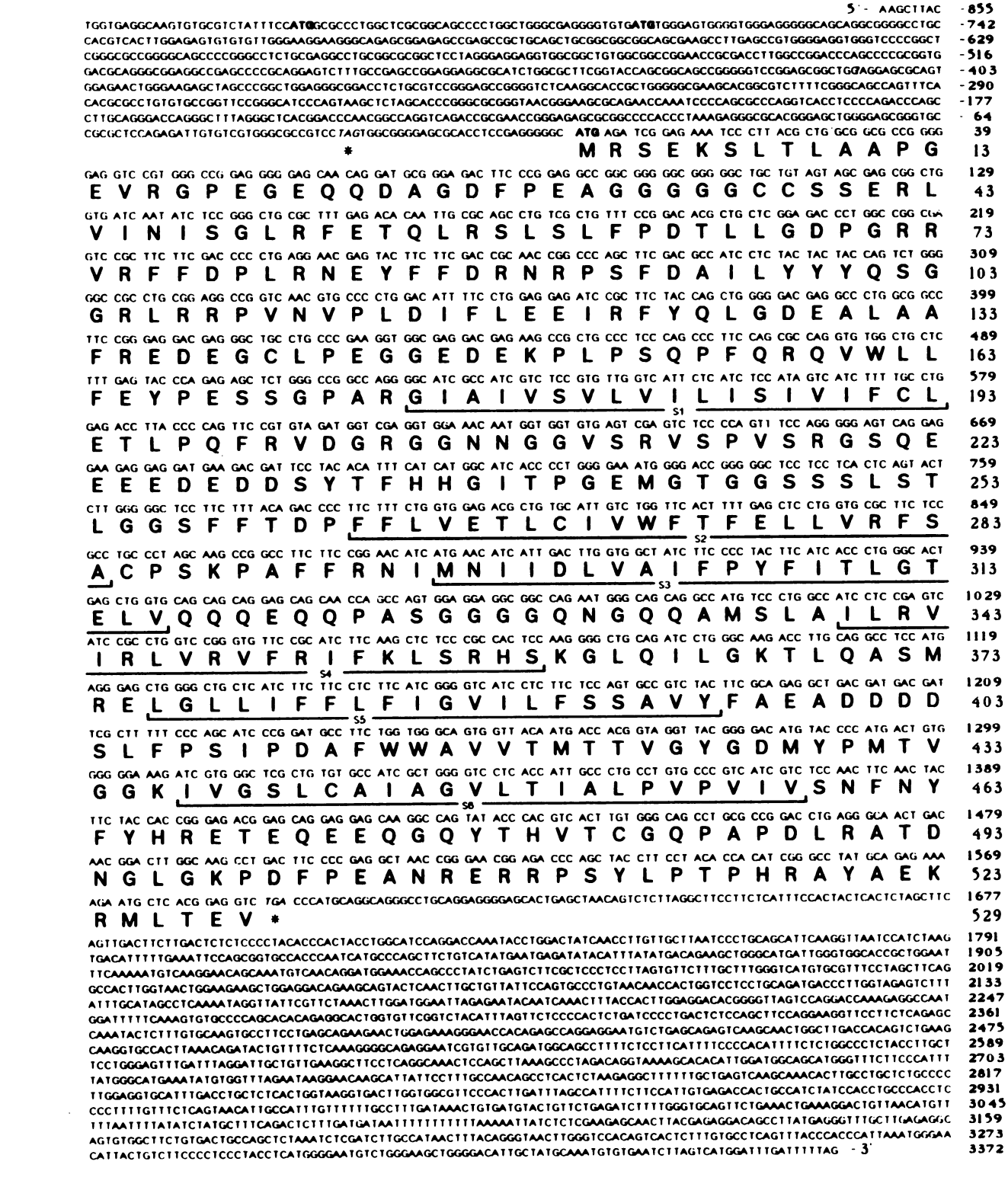

Fig. 1. DNA sequence and predicted amino acid sequence of the human K^+ channel forming protein HBK2. Nucleotides are numbered in the 5′−3′ direction, beginning with the first residue of the ATG triplet encoding the methionine initiation site. The nucleotides on the 5′ side of residue 1 are indicated by negative numbers. The number of the nucleotide residue at the right end of each line is given. The deduced amino acid sequence (in one-letter code) is shown below the nucleotide sequence. Amino acid residues are numbered beginning with the methionine initiation site. Numbers of the last residue are given on the right-hand side. The non-sense codon TGA at the end of ORF is marked by an asterisk. Proposed transmembrane segments S1−S6 are indicated by brackets. The segments are predicted from a hydropathy profile computed according to Kyte and Doolittle (1982). An asterisk in front of the first methionine denotes the first upstream in frame stop codon in the 5′-untranslated sequence. The sequence presented is a composite of genomic and cDNA clones. The sequence of cDNA clone H92 was from nucleotide +171 to +3372, that of the genomic clone HDTg from nucleotide −863 to +4092. The 3′-untranslated sequence of clone HDTg between nucleotides +3372 and +4092 is not shown.

Fig. 2. Alignment of the deduced human K^+ channel (HBK2) protein sequence with the deduced rat cortex K^+ channel (RCK2) protein sequence. Identical amino acid residues are indicated by bars. One gap has been introduced for maximal alignment of the two K^+ channel protein sequences between amino acid residues 210 and 211 of the HBK2 protein. Proposed transmembrane segments S1–S6 are indicated by brackets. The RCK2 sequence is deduced from a composite 2759 nucleotide long cDNA sequence. The sequence of cDNA R5050 was from nucleotide 1 to 1940, that of cDNA R5151 was from nucleotide 1093 to 2759.

labelled cDNA. The same results were obtained with genomic Southerns using human lymphocyte DNA or HeLa cell DNA. As described previously for RCK cDNAs, only a few hybridizing bands were observed with the differently cut genomic DNA (data not shown). This suggested that the corresponding gene is apparently present only once in the human haploid genome. A 5.0 kb *Hin*dIII restriction fragment, which hybridized with the N-terminal coding region of the cDNA, was selected for cloning and sequencing (see Materials and methods). The sequence of the genomic DNA was aligned with the cDNA sequence in order to derive a complete open reading frame (Figure 1). The genomic DNA sequence was co-linear with the cDNA sequence and contained only at two positions (out of 3600 nucleotides) a different nucleotide in the sequence. These differences would result in a conservative replacement of Ser58 (AGC) by Thr (ACC) and in a non-conservative replacement of Phe276 (TTT) by Ser (TCT). The combined genomic/DNA sequence information was used to derive a human K^+ channel protein sequence consisting of 529 amino acid residues with a calculated mol. wt of 58 891. Accordingly, the original cDNA sequence lacked 171 nucleotides (57 amino acids) at its 5′ end for derivation of a complete open reading frame (Figure 1). The derived protein sequence contains one potential N-glycosylation site (Asn46) and one potential phosphorylation site for protein kinases (Ser511). The proposed topology of K^+ channel proteins in the membrane would place both the sites on the intracellular side. Therefore, the potential N-glycosylation site at Asn46 is probably not used, suggesting that the deduced K^+ channel protein is not N-glycoslated.

The human K^+ channel is analogous to a novel member of the RCK protein family

The primary structure of the human K^+ channel is homologous to those of RCK (Stühmer *et al.*, 1989b) and *Shaker* (Kamb *et al.*, 1988; Pongs *et al.*, 1988; Schwarz *et al.*, 1988) K^+ channel subunits. However, unlike the known RCK or *Shaker* proteins, the derived sequence of the human K^+ channel subunit does not have a potential N-glycosylation site (N-X-S/T) in the bend region connecting the possibly membrane-spanning segments S1 and S2 (Figure 1). This and other features of the protein sequence (see below) suggested to us that the human K^+ channel subunit was related with a novel member of the RCK multigene family corresponding to another, not yet characterized RCK gene. We searched a rat cortex cDNA library for a related cDNA. Indeed, the search resulted in the isolation and characterization of another member of the RCK family (RCK2). Figure 2 aligns the derived amino acid sequences of the novel human and rat K^+ channel subunits. The human K^+ channel amino acid sequence has an overall identity of 94% versus the RCK2 amino acid sequence. We have therefore named the derived human K^+ channel sequence HBK2 (human brain K^+ channel 2), anticipating that the human genome harbours an HBK gene family (Kamb *et al.*, 1989) that is homologous in structure and complexity to the RCK gene family in the rat genome. A comparison of the HBK2 and RCK2 sequences shows that one insertion and 40 substitutions out of 529 amino acids have occurred between the human and the rat K^+ channel sequence. Most of these substitutions correspond to conservative amino acid replacements. Only 16 substitutions are non-conservative and are clustered mostly in the bend regions between possibly membrane-spanning segments S1–S2 and S3–S4 respectively. These regions of the K^+ channel have been suggested to face the extracellular side of the membrane.

HBK2 and RCK2 channels are also similar in hydropathy profiles (data not shown) to MBK and RCK channels (Baumann *et al.*, 1988; Tempel *et al.*, 1988; McKinnon, 1989; Stühmer *et al.*, 1989b), previously analysed, having five hydrophobic segments (S1, S2, S3, S5 and S6) and one positively charged segment (S4) containing a positively charged amino acid residue (arginine or lysine) at every third position. This scheme is like that found in every voltage-gated ionic channel, suggesting that the positive charges in the S4 segment are part of the voltage sensor (Stühmer *et al.*, 1989a). Based upon the topology previously proposed for voltage-gated K^+ channels (Pongs *et al.*, 1988), the amino- and carboxyl-terminal ends and the regions connecting segments S2–S3 and S4–S5 all reside on the cytoplasmic side of the membrane. The amino- and carboxyl-terminal

residues show low similarity to previously characterized K^+ channels. These sequences may be important for specifying distinct functional properties of vertebrate K^+ channels similar to the *Shaker* K^+ channel family (Iverson *et al.*, 1988; Timpe *et al.*, 1988a,b). Extracellular connecting sequences with low conservation (50−70%) are also found between segments S1−S2 and S3−S4. These sequences may be important for specifying distinct pharmacological properties of the K^+ channels. One major difference to the primary structure of previously characterized K^+ channels is that the S1−S2 bend region of HBK2/RCK2 K^+ channels is unusually long (70 amino acids) and rich in glycine/serine residues, reflecting a possible O-glycosylation instead of the N-glycosylation in the usually 10−30 amino acid long S1−S2 bend region of other cloned K^+ channels.

Expression of RCK2 mRNA in the nervous system

The size of RCK2 mRNA was estimated from Northern blot experiments (Figure 3A) using an RCK2-specific RNA probe derived from the 5′-non-translated sequence of RCK2 cDNA, which was very similar to the corresponding HBK2 DNA sequence. Of the 429 nucleotide long sequence in front of the first in-frame ATG of RCK2 cDNA, 72.3% were identical with the HBK2 DNA sequence. The hybridization with total RNA from rat brain of P30 animals yielded one specific band of ~6800 nucleotides which resisted RNase treatment. The probe hybridized to RNAs of smaller sizes, which is most likely due to unspecific hybridization, because these signals were seen in all tissues examined and in comparable amounts even in cases when the specific mRNA was not detected, such as in liver. Different amounts of the RCK2 transcript were detected in different areas of the central nervous system (Figure 3B). RCK2 mRNA was expressed most abundantly in medulla-pons and inferior colliculus (Figure 3B). Levels in superior colliculus and midbrain were comparable (not shown). Lower RCK2 mRNA levels were detected in corpus striatum (Figure 3B), cerebral cortex and hippocampus (not shown). Relatively minor amounts were found in RNA from cerebellum and spinal cord; the olfactory bulb expressed lowest levels. The RCK2 mRNA was detected at all developmental stages studied (E10−P90), which agrees with the isolation of HBK2 cDNA from a fetal human and of RCK2 cDNA from an adult rat cortex cDNA library. Apparently, the steady-state level of RCK2 mRNA increases until the end of the first postnatal week (Figure 3B) with sustained high levels until adulthood. RNA from dorsal root ganglia expressed levels of RCK2 mRNA comparable to total brain. As we have not detected RCK2 mRNA in RNA of skeletal muscle, heart muscle or liver, the expression of RCK2 mRNA seems to be specific for the nervous system. The expression of RCK2 mRNA exhibits a regional and temporal pattern in the central nervous system that is distinct from those of the other RCK family members (Beckh and Pongs, 1990).

Functional expression of HBK2 and RCK2 channels in Xenopus oocytes

The functional and pharmacological properties of the channels formed by RCK2 and HBK2 proteins were characterized after injection of RCK2 and HBK2 cRNAs into *Xenopus laevis* oocytes. K^+ currents mediated by RCK2 and HBK2 channels were recorded from macro-patches in the cell-attached configuration of the patch clamp method as described previously (Stühmer *et al.*, 1987, 1989b). The expressed K^+ channels were characterized by recording membrane currents in response to depolarizing voltage steps and measuring their voltage-dependent activation/inactivation properties and their single-channel amplitude.

Figure 4(A) shows a family of outward current traces mediated by HBK2 channels in response to steps in membrane voltage to various depolarizing test potentials. Following the voltage steps, the K^+ currents increased in a voltage-dependent manner (Table I). At 0 mV test potential it reached its maximum within a few milliseconds and then remained on a plateau during the 100 ms test pulses. The plateau value was voltage dependent and slightly saturated at positive membrane voltages. The currents mediated by RCK2 channels did not differ significantly from the HBK2 currents and are therefore not shown. In their time course and voltage dependence of activation the outward currents mediated by HBK2 and RCK2 channels resemble the currents mediated by RCK1 and RCK5 channels (Stühmer *et al.*, 1989b). However, the threshold of activation of HBK2/RCK2 channels was more positive (around −30 mV) than that of other RCK channels. Thus, unlike other expressed RCK channels, HBK2/RCK2 channels did not mediate outward currents in response to a step in membrane voltage from −80 to −40 mV.

Figure 4(B) shows the normalized conductance−voltage [G/G_{max} (V)] relation (steady-state activation curve) of the HBK2 channels for the peak responses. The HBK2 currents activated at test potentials that were more positive than −40 mV, and saturated at 30−40 mV. The conductances were half-maximal in the range of −30 to −8 mV (Table I), which was at more positive test potentials than the value determined for the steady-state activation of RCK1, RCK3, RCK4 and RCK5 channels (Stühmer *et al.*, 1989b). On the other hand, the slope of the conductance−voltage relation of the HBK2/RCK2 channels (d^n in Table I) was very similar to those of RCK1, RCK3 and RCK5 channels. The

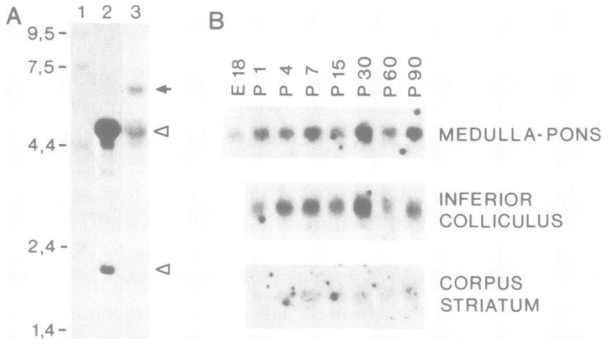

Fig. 3. Expression of RCK2 mRNA in the rat central nervous system. **(A)** Autoradiogram of RNA from rat brain of P30 animals hybridized to the RCK2-specific probe (**lane 3**), the methylene blue stained ribosomal RNAs (**lane 2**) and size markers (**lane 1**) which are indicated at the left-hand side in kb. The duration of autoradiography was 8 days. The RCK2 mRNA and the ribosomal 18S and 28S RNAs are indicated by closed and open arrowheads respectively. **(B)** Autoradiograms from RNA blot hybridization analysis of RNA from rat CNS regions given at the right-hand side of the corresponding Northern blot. The three selected regions exemplify forebrain, midbrain and hindbrain regions. The embryonic (E) and postnatal (P) stages of development are given on top of each lane in days. Hybridization and exposure times were as in (A). Only the RCK2-specific bands are shown.

activation time course, measured for the HBK2/RCK2 channels at 0 mV test potentials (Table I) was 18 ± 6 and 29 ± 16 ms, i.e. relatively slow compared to the other RCK channels. However, this is due to the right-shift of the activation curve in HBK2/RCK2 currents resulting in a slower rise time at the same membrane potential.

The time course of inactivation of the current mediated by HBK2 channels is illustrated in Figure 4(C). During a voltage step of 3.2 s to 0 mV the current mediated by HBK2 and RCK2 channels decreased to 75% of its maximal value (t^h in Table I). The values of t^h were between those determined for the inactivation of RCK1 and RCK5 channels (Stühmer *et al.*, 1989b). Since HBK2 and RCK2 channels needed several minutes for complete inactivation, a steady-state inactivation curve was not determined.

Figure 4(D) shows single-channel currents measured in two oocytes injected with HBK2 or RCK2 cRNA in response to voltage steps from −60 to 0 mV. The size of elementary currents was not significantly larger for HBK2 than for RCK2 channels (Table I). Both step sizes were in the same range as the single-channel current amplitudes of RCK1, RCK3 and RCK5 channels. The ion-selectivity for potassium of the HBK2/RCK2 channels was also in the same range as for RCK1, RCK3, RCK4 and RCK5 channels (see dV/P in Table I).

Table I. Functional characteristics of HBK2 and RCK2 channels

	$V^{n1/2}$ (mV)	a^n (mV)	t^n (ms)	t^h (%)	$i^{(0)}$ (pA)	dV/P (vM)
HBK2	−20.8 ± 7.5 (6)	−8.1 ± 1.5 (6)	18 ± 6 (6)	75 ± 3 (6)	0.91 (3)	56 (2)
RCK2	−17.3 ± 10.0 (4)	−6.1 ± 1.2 (4)	26 ± 19 (4)	72 ± 5 (3)	0.87 (4)	54 (1)

$V^{n1/2}$ refers to the test potential in mV where the conductance increase has reached one-half of its maximal value. The conductance was obtained as described in the legend of Figure 4(B).
a^n refers to the slope of the normalized conductance−voltage relation. Its value corresponds to the change in test potential (in mV) to cause an *e*-fold increase in conductance.
t^n refers to the rise-time of the K^+ currents (elicited by a step from −80 to 0 mV membrane potential) to reach 90% of amplitude.
t^h refers to ratio of peak amplitude to amplitude at the end of a 3.2 s voltage pulse to 0 mV test potential. Holding potential was −80 mV.
$i^{(0)}$ refers to the single-channel current amplitude in pA at 0 mV membrane potential. The respective chord conductances, assuming a reversal potential of −100 mV, are 8.7 and 9.1 pS respectively.
dV/P refers to the change in equilibrium potential caused by 10-fold change in K^+ concentration.

Pharmacology of HBK2 and RCK2 channels

The sensitivity of HBK2 and RCK2 channels to different K^+ channel blockers has been investigated in whole-cell current recordings using the two-microelectrode voltage clamp technique. The concentration dependence of the block of outward currents by a particular K^+ channel blocker was determined with voltage steps to 0 mV test potential. The concentrations needed for a 50% block of the outward current are summarized in Table II. The profile of the pharmacological sensitivity of HBK2 and RCK2 channels to the K^+ channel blockers 4-aminopyridine (4-AP), tetra-

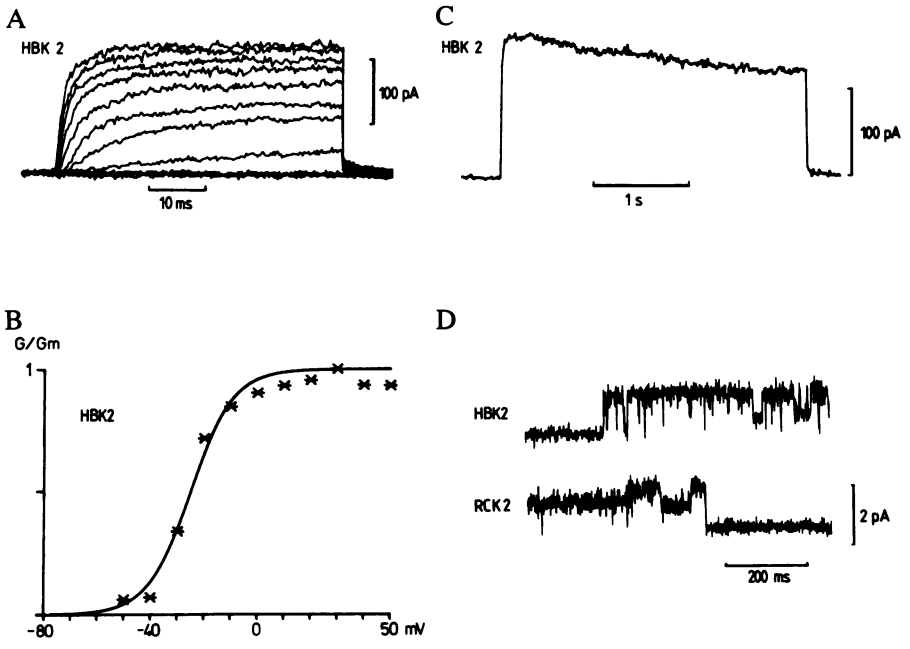

Fig. 4. Expression of HBK2 and RCK2 cRNAs in *Xenopus laevis* oocytes. (**A**) Family of outward K^+ currents mediated by HBK2 channels in response to depolarizing voltage steps of 100 ms from −80 mV to test potentials between −80 and +40 mV in 10 mV intervals. Ensemble currents were recorded from macro-patches. The records of two successive measurements have been averaged. Filtering at 3 kHz low pass, sampling at 5 kHz. (**B**) Plot of normalized conductance (G/G_{max}) versus test potential. To obtain the conductance values, the current maxima of the traces in (A) were divided by the difference between their test pulse potential and an assumed reversal potential of −100 mV. The line is the result of a non-linear least-squares fit of a Boltzmann isotherm to the normalized conductance. (**C**) Time course of inactivation of currents mediated by HBK2 channels during a 3.2 s depolarizing test pulse from −80 mV to 0 mV. The trace is an average of three. Filtering at 120 Hz low pass, sampling at 62.5 Hz. (**D**) Single-channel recordings of HBK2 and RCK2 channels. Both current traces were recorded during a prolonged depolarization of a cell-attached patch after a voltage step from −60 mV to 0 mV. The mean single-channel amplitude of HBK2 channels was slightly, but not significantly higher (0.91 pA) than the one of RCK2 channels (0.87 pA). Both channel types showed substates in their elementary currents of almost one half of their total current amplitude. Upward deflection corresponds to channel opening. Filtering at 1 kHz low pass, sampling at 2 kHz.

Table II. Action of K^+ channel blockers on HBK2 and RCK2 channels

	Blocker					
	4-AP (mM)	TEA (mM)	DTX (nM)	MCDP (nM)	CTX (nM)	β-BUTX (nM)
HBK2, RCK2	1.5	7	20	10	1	⩾200

The concentrations given refer to the ID_{50} values (50% inhibition of peak current, measured at 0 mV; experiments were made in a two-microelectrode voltage clamp configuration). The sign '⩾' indicates no effect at the highest concentration tested.

ethylammonium (TEA), dendrotoxin (DTX), charybdotoxin (CTX), mast cell degranulating peptide (MCDP) and β-bungarotoxin (β-BTX) was identical, but different from all other RCK channels (Stühmer *et al.*, 1989b). The HBK2 and RCK2 channels were as sensitive to CTX and to 4-AP as RCK3 channels but much more sensitive to TEA and to DTX than RCK3 channels. On the other hand, their sensitivity to TEA and DTX was low compared to RCK1 channels. This indicates that each member of the RCK gene family has its own pharmacological profile.

Discussion

The HBK2 channels and its rat homologue RCK2 represent a novel member of the RCK gene family (Stühmer *et al.*, 1989b), extending the number of different RCK K^+ channels to five. The RCK2/HBK2 K^+ channels have functional and pharmacological properties distinct from the RCK1, RCK3, RCK4 and RCK5 channels. The functional characteristics are that of a typical delayed-rectifier channel (Rudy, 1988), which acts especially in the more positive membrane voltage range. Although the derived RCK2 and HBK2 protein sequences differ at 40 positions, the whole spectrum of properties found in HBK2 cRNA expressing *Xenopus* oocytes is reproduced in RCK2 cRNA expressing oocytes, demonstrating that the amino acid replacements between the rat and human K^+ channel proteins are not significant for its function. As described in Results, the HBK2 cDNA sequence was completed by a corresponding genomic DNA sequence that was co-linear with the cDNA sequence. It is presently not clear whether this co-linearity indicates that the HBK2 open reading frame is not interrupted by intervening sequences or whether the human genome contains K^+ channel pseudogenes. Although our whole genome Southern analysis does not indicate the existence of HBK2 pseudogenes, the complete cloning of the HBK2 gene is required to resolve this question.

A comparison of the deduced RCK2/HBK2 protein sequences with the *Shaker* (Kamb *et al.*, 1988; Pongs *et al.*, 1988; Schwarz *et al.*, 1988) and the other RCK protein sequences indicates that a pattern is now emerging for the different members of the *Shaker*/RCK proteins. The general structure among these voltage-gated K^+ channel proteins is highly conserved, with six possibly membrane-spanning segments preceded by a conserved sequence of 130 amino acids on the N-terminal side. The N-terminal sequences can vary in length and in sequence considerably, whereas the C-terminal sequences are also variable, but always possess a potential phosphorylation site for serine/threonine protein kinases (Rehm *et al.*, 1989). Current topological models of the K^+ channels in the membrane place the bend regions between segments S1–S2, segments S3–S4 and segments S5–S6 on the extracellular side. In agreement with this view of the K^+ channel structure is the observation that these bend regions are not well conserved among the members of the *Shaker*/RCK K^+ channel family, whereas the bend regions between segments S2–S3 and S4–S5, presumably located at the intracellular side of the membrane, are highly conserved. The HBK2/RCK2 K^+ channels are the first ones that do not have a potential N-glycosylation site in the bend region between segments S1–S2. They might be O-glycosylated instead because this bend region is rich in glycine/serine residues. RCK1, RCK3, RCK4 and RCK5 bend regions are 39 ± 5 amino acids long and do not have an excess of negatively or positively charged amino acids. The RCK2/HBK2 bend regions, on the contrary, are 69/70 amino acids long, i.e. almost twice the size of those of the other RCK channels. Also, they exhibit an excess of seven negatively charged amino acid residues. However, the basic electrophysiological properties of the HBK2/RCK2 channels in the oocyte expression system are quite similar to those of the RCK1, RCK3 and RCK5 channels (Stühmer *et al.*, 1989b). This suggests that neither the distance between segments S1 and S2 nor the charge of the sequence connecting these two segments seems to influence profoundly the K^+ channel properties.

The affinity of the positively charged toxins DTX and CTX, which block K^+ channels from the outside, would depend on the number and kind of negatively charged amino acids being near or in the mouth of the K^+ channel (McKinnon and Miller, 1989). Therefore, we have suggested previously that the CTX sensitivity of an RCK channel could be correlated with the number of acidic amino acid residues in the S3–S4 bend region and the DTX sensitivity with the presence of an acidic amino acid residue (Asp402) in the S5–S6 bend region (Stühmer *et al.*, 1989b). The pharmacology of the HBK2/RCK2 channels expressed in *Xenopus* oocytes (Table II) is in agreement with our previous suggestion.

Biochemical work has shown that two populations of DTX acceptors, associated with neuronal K^+ channels, were discernible in preparations of chick synaptic membranes (Black and Dolly, 1986) and of rat brain membranes (Rehm and Lazdunski, 1988). The two DTX-acceptor subtypes bind β-BTX either with low or high affinity. Apparently, this latter class of DTX and β-BTX binding K^+ channels has not been cloned yet. Given the structural similarities among the variant K^+ channels that have been cloned and characterized so far, it can be expected, however, that β-BTX sensitive K^+ channels have a very similar primary structure.

Materials and methods

Screening of cDNA libraries

A human fetal cDNA library kindly provided by P.Seeburg (ZMBH, Heidelberg) was screened at low stringency according to Benton and Davis (1977) with a labelled probe derived from RCK3 cDNA. Similarly, an adult rat brain cDNA library was screened with a labelled probe derived from HBK2 cDNA. The hybridization was performed in 5 × SSC (20 × SSC is 3 M sodium chloride, 0.3 M sodium citrate, pH 7.0), 0.1% bovine serum albumin, 0.1% Ficoll, 0.1% polyvinyl pyrrolidone, 100 μg/ml denatured salmon sperm DNA, 50 mM sodium phosphate (pH 7.0), 0.1% SDS, 43% deionized formamide at 37°C for 12 h (McGinnis *et al.*, 1984). Filters were

washed twice in 2 × SSC, 0.1% SDS for 5 min at room temperature, followed by two washes for 15 min each at 42°C. Recombinant DNA was propagated in ER1 host−vector system under L2 containment conditions, as defined in the guidelines of the Federal German Government for recombinant DNA research. Recombinant DNA was isolated according to Maniatis *et al.* (1982). ^{32}P-labelled DNA probes were prepared with an oligonucleotide labelling kit (Boehringer).

Cloning of genomic HBK2 DNA

Genomic DNA of HeLa cells digested with *Hin*dIII was separated by agarose gel electrophoresis (Maniatis *et al.*, 1982). A 5 kb *Hin*dIII band that hybridized with HBK2 cDNA was cut out of the gel and isolated (Vogelstein and Gillespie, 1979). The *Hin*dIII fragment was ligated with *Hin*dIII-cut λNM1149. Recombinant phages were packed *in vitro* (Gigapack Gold, Stratagene) and plated on the *Escherichia coli* POP13b strain (Shull *et al.*, 1986). Positive phages were selected after hybridization with radiolabelled HBK2 cDNA. Inserted HeLa DNA was subcloned into Bluescript.

Restriction maps and sequencing

Restriction maps were derived by a combination of complete, single and double digests followed by gel electrophoresis of the resulting fragments on 0.7% agarose gels (Maniatis *et al.*, 1982). cDNAs were subcloned into Bluescript and deletions were generated with DNase I according to Lin *et al.* (1985). Deleted subclones were selected after plasmid mini-preparation, restriction digestions and agarose gel electrophoresis. The dideoxy nucleotide sequencing technique was used for sequencing both strands of overlapping cDNA subclones (Sanger *et al.*, 1977).

Northern blots

A detailed description of the preparation of CNS tissues is given in Beckh *et al.* (1989). Total RNA was isolated by the guanidine thiocyanate method (Chirgwin *et al.*, 1979). Each RNA sample was adjusted to a concentration of 2.5 μg/μl. RNA (7.5 μg) was applied to each lane. Northern blot experiments were as described (Beckh *et al.*, 1989). The probe was prepared from a KS^+ Bluescript subclone of a *Hin*dIII−*Sac*I fragment of RCK2 cDNA (nucleotides −430 to −47) by T7 polymerase (Stratagene) promoted transcription using [α-^{32}P]UTP. The sp. act. of the probe was 5×10^8 d.p.m./μg. Hybridization was carried out in 50% formamide at 68°C (Thomas, 1980). Washing of blots was in 0.1 × SSC and 0.1% SDS at 70°C with several changes of buffer. Autoradiography was performed at −80°C with an intensifying screen. An RNA ladder (Bethesda Research Laboratories) was used as size markers.

Current recording and data analysis

Electrophysiological experiments were done with *X.laevis* oocytes 4 days after microinjection of HBK2 or RCK2 cRNA (Stühmer *et al.*, 1989b). All experiments were performed in a bathing solution containing (in mM) NaCl 115, KCl 2.5, $CaCl_2$ 1.8, HEPES 10 (pH 7.2). In some experiments, sodium was partly replaced by potassium or blocking substances [TEA and 4-AP (Sigma), β-BTX, DTX (gift from Drs F.Dreyer and E.Habermann, Universität Giessen, FRG) and MCDP (Bachem, Bissendorf Biochemicals, Hannover, FRG), charybdotoxin (gift from Dr C.Miller, Brandeis University, USA)] added to the bathing solution. A two-microelectrode voltage clamp was used to test for the action of the K^+ channel blockers and to determine the whole-cell K^+ current of each oocyte prior to patch current recording. In ~20% of the oocytes injected with HBK2 or RCK2 cRNA the current was >10 μA at 0 mV test potential. This indicated that the channel density was high enough to obtain smooth current traces in ensemble current records from cell-attached patches.

Patch pipettes were filled with the normal bathing solution in all experiments. Pipettes for macro-patches were made from aluminum-silicate glass and had a tip diameter of 6 μm and a resistance of 0.5−1 MΩ when filled with bathing solution. The intracellular potential was simultaneously measured by a second microelectrode to monitor the transmembrane potential across the patch. To find the area of maximal channel density the oocyte was turned around by an angle of 90° between the first three patch experiments. Stimulation and sampling was done by a VME-bus computer. Leak and capacitive currents were subtracted on-line using the P/4 procedure. To determine the steady-state activation parameters, the parameters $V^{n1/2}$, a^n and G_{max} of a single Boltzmann isotherm of the form

$$G = G_{max}/\{1+\exp[(V - V^{n1/2})/a^n]\}$$

were fitted to the peak values of a family of records. To get the conductance (G) the peak current values were divided by the driving potential assuming a reversal potential of −100 mV.

Pipettes for single-channel recording were made from borosilicate glass, and had a diameter of 1 μm and resistances of 3−5 MΩ when filled with bathing solution. The single-channel current records were stored on video tape and analysed by an interactive semi-automatic procedure. Distribution of single-channel current amplitudes were fitted by either single or sums of Gaussians.

Acknowledgements

We thank Drs F.Dreyer and E.Habermann for the generous gift of DTX, Dr C.Miller for the generous gift of CTX and Professor E.Neher, Göttingen, for his hospitality to S.B. The work was supported by grants and the Leibniz-Förderprogramm of the DFG. The sequence data will appear in the EMBL/Gen Bank/DDBJ/Nucleotide Sequence Databases [accession numbers X17621 (RCK2) and X17622 (HBK2)].

References

Baumann,A., Grupe,A., Ackermann,A. and Pongs,O. (1988) *EMBO J.*, **7**, 2457−2463.
Beckh,S. and Pongs,O. (1990) *EMBO J.*, **9**, 777−782.
Beckh,S., Noda,M., Lübbert,H. and Numa,S. (1989) *EMBO J.*, **8**, 3611−3616.
Benton,W.D. and Davis,R.W. (1977) *Science*, **196**, 180−182.
Black,A.R. and Dolly,J.O. (1986) *Eur. J. Biochem.*, **156**, 609−617.
Butler,A., Wei,A., Baker,K. and Salkoff,L. (1989) *Science*, **243**, 943−947.
Chirgwin,J.M., Przybyla,A.E., MacDonald,R.J. and Rutter,W.J. (1979) *Biochemistry*, **18**, 5294−5299.
Frech,G.C., Van Dongen,A.M., Schuster,G., Brown,A.M. and Joho,R.H. (1989) *Nautre*, **340**, 642−645.
Hille,B. (1984) *Ionic Channels in Excitable Membranes*. Sinauer, Sunderland, MA.
Iverson,L.E, Tanouye,M.A, Lester,H.A., Davidson,N. and Rudy,B. (1988) *Proc. Natl. Acad. Sci. USA*, **85**, 5723−5727.
Kamb,A., Tseng-Crank,J. and Tanouye,M.A. (1988) *Neuron*, **1**, 421−430.
Kamb,A., Weir,M., Rudy,B., Varmus,H. and Kenyon,C. (1989) *Proc. Natl. Acad. Sci. USA*, **86**, 4372−4376.
Kyte,J. and Doolittle,R.F. (1982) *J. Mol. Biol.*, **157**, 105−132.
Lin,H.C., Lei,S.P. and Wilcox,G. (1985) *Anal. Biochem.*, **147**, 114−119.
MacKinnon,R. and Miller,C. (1989) *Science*, **245**, 1382−1385.
Maniatis,T., Fritsch,E.F. and Sambrook,J. (1982) *Molecular Cloning: A Laboratory Manual*. Cold Spring Harbor Laboratory Press, Cold Spring Harbor, NY.
McGinnis,W., Levine,M.S., Hafen,W., Kuroiwa,A. and Gehring,W.J. (1984) *Nature*, **308**, 428−433.
McKinnon,D. (1989) *J. Biol. Chem.*, **264**, 8230−8236.
Pongs,O., Kecskemethy,N., Müller,R., Krah-Jentgens,I., Baumann,A., Kiltz,H.H., Canal,I., Llamazares,S. and Ferrus,A. (1988) *EMBO J.*, **7**, 1087−1096.
Rehm,H. and Lazdunski,M. (1988) *Proc. Natl. Acad. Sci. USA*, **85**, 4919−4923.
Rehm,H., Pelzer,S., Cochet,C., Chambaz,E., Tempel,B.L., Trautwein,W., Pelzer,D. and Lazdunski,M. (1989) *Biochemistry*, **28**, 6455−6460.
Rudy,B. (1988) *Neuroscience*, **25**, 729−750.
Sanger,F., Nicklen,S. and Coulson,A.R. (1977) *Proc. Natl. Acad. Sci. USA*, **74**, 5463−5467.
Schwarz,T.L., Tempel,B.L., Papazian,D.M., Jan,Y.N. and Jan,L.Y. (1988) *Nature*, **331**, 137−142.
Shull,G.E., Goceb,J. and Lindgrel,J.B. (1986) *Biochemistry* **25**, 8125−8132.
Stühmer,W., Methfessel,C., Sakmann,B., Noda,M. and Numa,S. (1987) *Eur. Biophys. J.*, **14**, 131−138.
Stühmer,W., Stocker,M., Sakmann,B., Seeburg,P., Baumann,A., Grupe,A. and Pongs,O. (1988) *FEBS Lett.*, **242**, 199−206.
Stühmer,W., Conti,F., Suzuki,H., Wang,X., Noda,M., Yahagi,N., Kubo,H. and Numa,S. (1989a) *Nature*, **339**, 597−603.
Stühmer,W., Ruppersberg,J.P., Schröter,K.H., Sakmann,B., Stocker,M., Giese,K.P., Perschke,A., Baumann,A. and Pongs,O. (1989b) *EMBO J.*, **8**, 3235−3244.
Tempel,B.L., Jan,Y.N. and Jan,L.Y. (1988) *Nature*, **332**, 837−839.
Thomas,P.S. (1980) *Proc. Natl. Acad. Sci. USA*, **77**, 5201−5205.
Timpe,L.C., Jan,Y.N. and Jan,L.Y. (1988a) *Neuron*, **1**, 659−667.
Timpe,L.C., Schwarz,T.L., Tempel,B.L., Papazian,D.M., Jan,Y.N. and Jan,L.Y. (1988b) *Nature*, **331**, 143−145.
Vogelstein,B. and Gillespie,D. (1979) *Proc. Natl. Acad. Sci. USA*, **76**, 615−619.

Received on January 31, 1990; revised on March 13, 1990